

# Development and characterization of sol–gel silica–alumina composite coatings on AISI 316L for implant applications

S.K. Tiwari\*, T. Mishra, M.K. Gunjan, A.S. Bhattacharyya, T.B. Singh, R. Singh

*National Metallurgical Laboratory, Jamshedpur-831007, India*

Received 10 October 2006; accepted in revised form 15 February 2007

Available online 23 February 2007

## Abstract

Sol–gel alumina coatings were deposited on medical grade stainless steel (AISI 316L) with an intermediate layer of silica by dip-coating method. The coatings obtained were homogeneous, crack-free and consisted of low crystalline  $\gamma$ - $\text{Al}_2\text{O}_3$  along with some boehmite phase. EDAX revealed the presence of only Al in the film. The corrosion performance of alumina-coated stainless steel was evaluated by electrochemical polarization, open-circuit potential measurement and chronoamperometry in Ringer's solution. Coating has shown to enhance the pitting potential of AISI 316L by  $\sim 470$  mV and reduced passive current  $\leq 10^{-9}$  A  $\text{cm}^{-2}$ . The formation of thermodynamically stable silica–alumina interface was proposed to account for enhanced corrosion protection behaviour of the coating.

© 2007 Elsevier B.V. All rights reserved.

*Keywords:* Stainless steel; Coating; Sol–gel; Aluminium oxide; Corrosion resistance; Biointerface

## 1. Introduction

Metallic materials such as Ti, Ti-alloy, Co–Cr alloy and stainless steel (AISI 316L) are used as biomaterials due to their superior tensile and fatigue strength, and fracture toughness as compared to nonmetals such as polymeric and ceramic [1]. However, metallic materials corrode by aggressive biofluid and release metallic ions which resulted in the reduction of their biocompatibility. The biocompatibility and corrosion resistance of these implants are primarily determined by their constituent material and surface micro structural properties such as roughness, grain size, etc. Among the metallic materials, AISI 316L stainless steel is most commonly employed for temporary devices such as fracture plates, bone screws and hip nails due to its low cost and acceptable biocompatibility [2,3]. However, it has been often reported to suffer from severe crevice and galvanic corrosion, primarily due to the presence of occluded sites and high chloride concentration in physiological fluid [4]. The corrosion of the stainless steel implant releases metal ions such as Fe, Ni and Cr, which produce local systematic effects

and thereby plays a role in prosthetic loosening. A study showed that AISI 316L stainless steel produces corrosion products above certain non-lethal concentrations and thereby disturb the proliferation/differentiation relationship of osteoblastic human alveolar bone cell cultures in a dose dependent manner [5]. Therefore, major interest in stainless steel research has now been focused on to improve corrosion resistance (localized and generalized mechanism) and to prevent the metal ions from diffusing to nearby tissues. Furthermore, adhesion between implant and bone would not be desirable to avoid difficulty during removal of the implant (temporary) after the service.

A simple way of preventing corrosion or metal ion diffusion may be a hermetic sealing of the surface with materials stable against diffusion of corrosive species such as water, oxygen, acids, bases or combination of them. Various surface modification techniques, such as plasma ion implantation [6–8], laser melting [9–11] and laser surface alloying [12,13], physical and chemical vapor deposition (PVD and CVD) [14,15], thermal oxidation [16], electrochemical surface modification/anodizing [17], have been tried out to improve wear, corrosion, and fretting resistance of orthopaedic implants. However, each of these methods has limitations concerning the performance of tailored surfaces and their complex operating procedures. Sol–gel thin

\* Corresponding author. Tel.: +91 657 2271709-14x2101.

E-mail address: [drsktb@rediffmail.com](mailto:drsktb@rediffmail.com) (S.K. Tiwari).

film processing represents an alternative method to obtain the desired coatings [18]. The attractiveness of the process lies in tailoring functional properties of coatings by changing precursors, thermal treatments or addition of particles in sol. The main advantage of the process is the ability to form inorganic structures at a relatively low temperature and to produce thin homogeneous films on large scale [19].

Efforts have been made to enhance the corrosion resistance of metallic implants by depositing  $ZrO_2$  [20,21], silica [22–24], alumina [25–27], etc., through sol–gel route. Amongst these, alumina particularly appears promising due to its high resistance to wear, corrosion, and good thermal barrier properties [28]. Masalski et al. [26] obtained amorphous  $Al_2O_3$  film on AISI 316L stainless steel through sol–gel dip-coating followed by heating at 500 °C; coating showed to be stable during 1000 h of exposure in Ringer's solution. The potentiodynamic results, however, showed severe fluctuations in current, indicating instability and less protective coating at higher electrochemical potentials. It seems that the stable interface between coating and substrate is essential for coating to be better stable that may isolate the underlying metal from corrosive solution. It has been observed [29] that alumina silica mixed compounds has much lower free energy values than the boehmite. This leads to the concept that an alumina/silica interface should be thermodynamically stable against corrosion.

Keeping above facts in view, attempts have been made to deposit  $SiO_2/Al_2O_3$  film on AISI 316L through sol–gel route with an intent to enhance the stability of coating to improve localized corrosion resistance of AISI 316L for biomedical applications. The stable composite coating was also aimed to prevent leaching of undesirable metallic elements from going into the solution, essential for biocompatible coating. The coatings obtained were characterized for homogeneity by SEM and AFM. The chemical composition of the coating was analyzed by EDAX. Adherence of coating was determined by scratch test method. The purity and phases were analyzed through FTIR and XRD. The coated 316L samples were evaluated for corrosion resistance in physiological conditions through open circuit potential measurement, polarization tests and chronoamperometry. The solution after corrosion tests was subjected to metal ions analyses for possible leaching and compared with the uncoated AISI 316L.

## 2. Experimental procedure

### 2.1. Sample preparation

Stainless steel 316L (elemental composition in wt.%: C—0.03, Cr—18.0, Ni—12.0, Mo—2.45, Mn—1.70, P—0.04, S—0.01, Si—0.16, Fe—Bal.) was selected as substrate, as it is commonly used for biomedical application. Solution annealed SS plate was cut into 25 mm×10 mm×3 mm size coupons. Coupons were polished using silicon carbide papers ranging from 120–1200 grit. The polished specimens washed with detergent solution, degreased with acetone and thoroughly washed with distilled water, were kept in ethanol before coating.

### 2.2. Preparation of sol and coating

Aluminium isopropoxide (ACROS) and tetraethyl–orthosilicate (Aldrich) were used as source of  $Al_2O_3$  and  $SiO_2$ , respectively. The alumina sol was prepared by hydrolysis and poly condensation of aluminium isopropoxide catalysed by  $HNO_3$  as reported elsewhere [26]. The ethanolic silica sol was prepared by mixing silane (TEOS) with ethanol and water: silane/distilled water/ethanol=5/5/90% (v/v). Both sols were kept at least for four days with intermittent stirring before coating. Before alumina coating, the AISI 316L specimens kept in ethanol were dipped in silica sol, withdrawn slowly (0.5 mm/s) and dried at 100 °C. The process was repeated two times. The  $Al_2O_3$  coatings were deposited on  $SiO_2$  coated specimen by dip-coating technique at a pulling speed of 0.8 to 1 mm/s. Dip-coated samples were dried in air before heating at 300 °C for 15 min. The process of deposition, drying and heat treatment were repeated four times to increase the thickness of coating and finally heated at 500 °C for 2 h.

### 2.3. Physical characterization and adhesion test

The sol was dried at 100 °C in an oven for 48 h. The solid phase content was grind and heated at 500 °C for 2 h to get similar phase as in the coating. The phase composition of the powder, heated at 500 °C, was determined by X-ray diffractometer (XRD, SIEMENS, D-500) using a  $Cu-K_{\alpha}$  radiations. The diffraction intensity was measured by the scanning technique in the range of  $2\theta=4^{\circ}-70^{\circ}$ . FTIR spectra was recorded using a NICOLET-7500 spectrometer in the wave number ranging from 400 to 4000  $cm^{-1}$ , with KBr pellets. The topography of the coating on AISI 316L was studied by using Scanning Electron Microscopy (JEOL 840A, Japan) and Atomic Force Microscopy (AFM, SPA-400, SEIKO, Japan). Composition of the film was obtained through EDAX. Coating thickness and the roughness of the film was determined by means of Taylor Hobson surface profilometer.

Adhesion test was carried out by driving a Rockwell C diamond indenter (120° angle, 200  $\mu m$  radius) using computer controlled scratch tester (Model TR101, DUCON). The specimen was mounted on the test table, which was slid at a speed of 0.2 mm/s. The load on the indenter was increased linearly at a rate of 10 N/mm.

### 2.4. Electrochemical characterization

Electrochemical measurements were made in Ringer's solution prepared by adding 9 g/l NaCl, 0.17 g/l  $CaCl_2$ , 0.42 g/l KCl, and 2.0 g/l  $NaHCO_3$  (AR grade chemicals) to distilled water. The pH of the solutions was maintained by adding requisite amount of NaOH or HCl. Polarization data were generated using a computer controlled Potentiostat/Galvanostat (Gamry Instruments, USA). The corrosion test cell was the classic configuration of three electrodes (graphite as counter, a saturated calomel electrode as reference and the coated metallic sample as working electrode). Polarization curves were obtained by a potential sweep in the noble direction at a constant

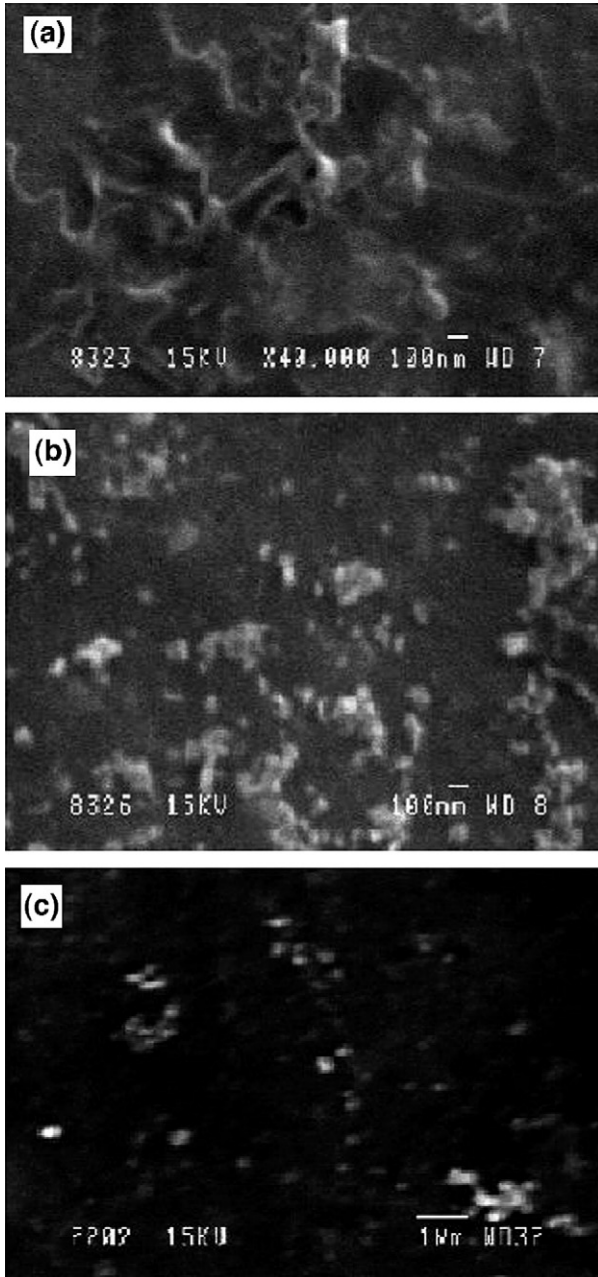


Fig. 1. Topography of  $\text{SiO}_2/\text{Al}_2\text{O}_3$  coating on AISI 316L heated at (a) 500 °C; (b) 700 °C; (c) 500 °C followed by exposure to Ringer's solution for 100 h.

controlled rate of 0.5 mV/s, starting at  $-100$  mV below the open circuit potential (previously stabilized). The pitting behaviour and stability of the coating was monitored by polarizing the electrode up to 800 mV in anodic direction and reversing the scan thereafter. After completion of the experiment, the open circuit potential of the electrode was monitored for 100 h and finally cyclic polarization curve was again recorded, to see the stability of coating. The leaching of metal ions was studied by chronoamperometry. The coated as well as uncoated electrodes were exposed at constant potential for 40 min and the resulting current was recorded. After completion of the experiment, the experimental solution was

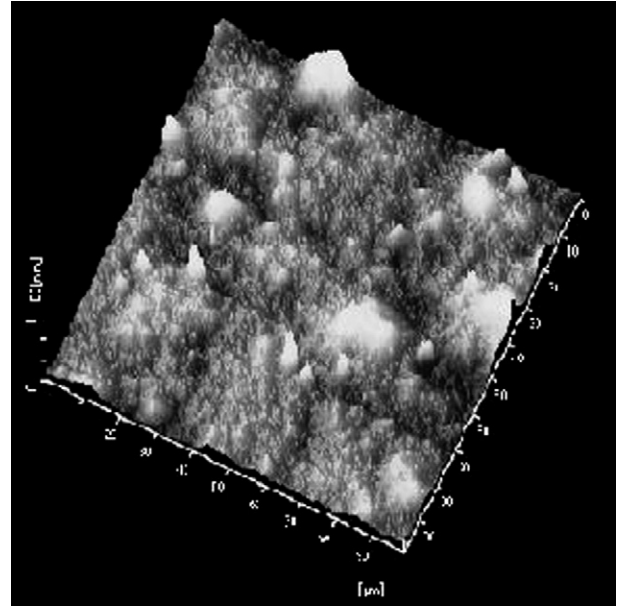


Fig. 2. AFM image of  $\text{SiO}_2/\text{Al}_2\text{O}_3$  films on AISI 316L heated at 500 °C.

analyzed by ICP spectroscopy for iron, nickel, chromium and manganese content.

### 3. Results and discussion

#### 3.1. Characterization

Coatings on stainless steel substrate with metal oxides present several advantages compared to non-coated metal such as resistance against corrosion and oxidation or coloration. Alumina was obtained in four coating cycles with prior coat of silica on stainless steel. The thickness and roughness of the coating as determined from surface profilometer after final heat treatment at 500 °C was found to be  $0.35 \pm 0.03 \mu\text{m}$  and  $0.07 \mu\text{m}$ , respectively. The scanning electron micrographs in Fig. 1 a–c showed featureless surface and no well defined grains. Morphology of coating given in Fig. 1a–c confirms it to

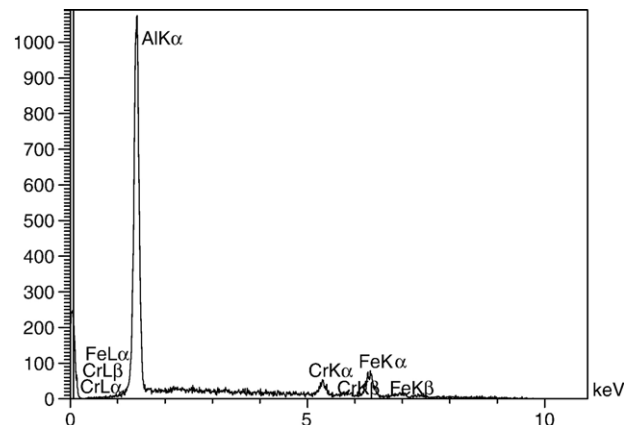


Fig. 3. EDX spectrum of  $\text{SiO}_2/\text{Al}_2\text{O}_3$  films on AISI 316L heated at 500 °C.

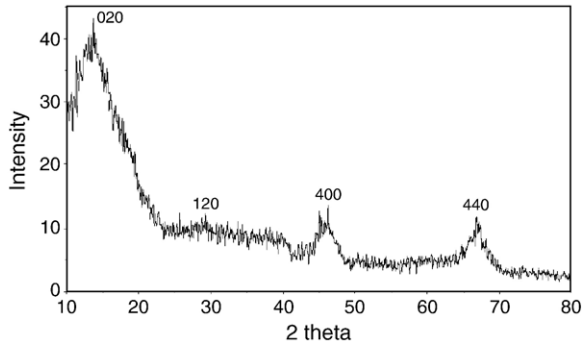


Fig. 4. Diffraction pattern of dried alumina gel powder heated at 500 °C for 2 h.

be homogeneous and crack-free. Heating at higher temperature (700 °C for 2 h) also did not indicate any structural change in the coating (Fig. 1b). No deterioration in the coating was visible and it remained intact even after 100 h of exposure to Ringer's solution followed by cyclic polarization (Fig. 1c). AFM analysis indicated coating consisting of self-agglomerated nanoparticles without any defects (Fig. 2). The EDAX analysis of the film indicated the presence of Al along with small amount of Cr and Fe (Fig. 3). The small amount of Cr and Fe indicated in the film may be originated from substrate due to penetration of X-rays as the film thickness is less than 0.5  $\mu\text{m}$ .

X-ray diffractogram of gel powder heated at 500 °C (Fig. 4) showed two  $\gamma$ -alumina peaks, (400) and (440) [ICDD, File 29-63] along with (020) and (120) peaks of boehmite. This suggests that the boehmite was not fully transformed to  $\gamma$ -alumina at 500 °C. The grazing incidence (GI) XRD of coated AISI 316L also indicated the presence of  $\gamma$ -alumina (as observed in Fig. 4) in addition to base alloy. The FTIR spectra of powder, obtained by drying sol at 100 °C and heated at 500 °C are shown in Fig. 5. IR spectra of the sample dried at 100 °C exhibited a band at 1072  $\text{cm}^{-1}$  with a shoulder at 1162  $\text{cm}^{-1}$ , which are attributed to the symmetrical and anti symmetrical AlOH bending modes. The stretching Al–O modes of  $\text{AlO}_6$  groups are found below 900  $\text{cm}^{-1}$  (894, 737 and 638  $\text{cm}^{-1}$ ). The two broad bands at 894 and 494  $\text{cm}^{-1}$  in the sample treated at 500 °C are attributed to two coordinations of Al atoms in  $\gamma\text{-Al}_2\text{O}_3$  [29]. The band at

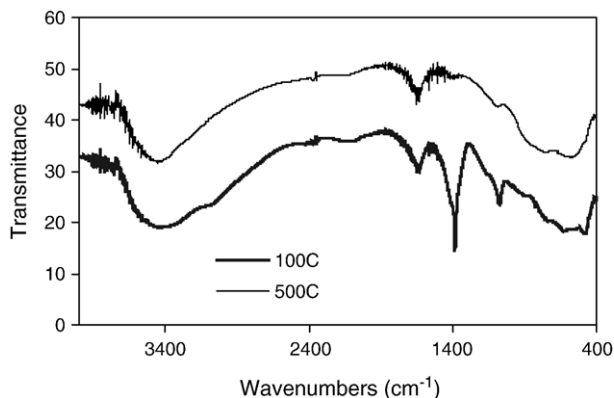


Fig. 5. FTIR spectra of alumina gel samples heated for 2 h at (a) 100 °C and (b) 500 °C.

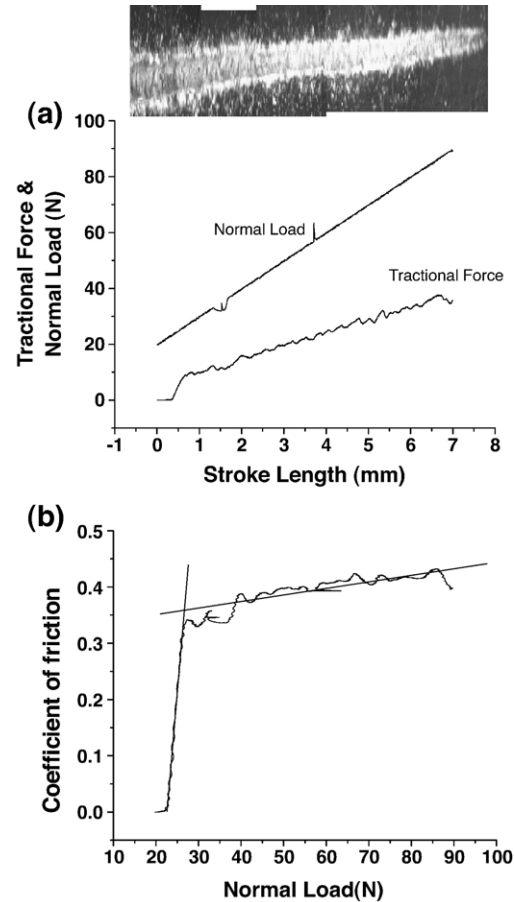


Fig. 6. Scratch test on  $\text{SiO}_2/\text{Al}_2\text{O}_3/\text{AISI 316L}$  heated at 500 °C for 2 h. (a) Tangential and Normal load as a function of scratch length; (b) Coefficient of friction vs Vertical load.

1390  $\text{cm}^{-1}$ , which disappeared after heating at 500 °C corresponds to  $\text{NO}_3^-$  group from  $\text{HNO}_3$  added for peptization. The absorption band at 1650  $\text{cm}^{-1}$  appeared in both samples is due to moisture in the sample [30]. Hence the IR data also support the XRD pattern suggesting the partial formation of  $\gamma\text{-Al}_2\text{O}_3$ .

The durability and functionality of film is critically dependent on the adhesion between the film and the underlying substrate. The results of adhesion of the coating to AISI 316L, determined by scratch test are shown in Fig. 6. Fig. 6a displays applied normal load and resulting tangential force as function of scratch track length for  $\text{SiO}_2/\text{Al}_2\text{O}_3$  coating on AISI 316L heated at 500 °C. The first part where the applied normal load is less than the critical load, a linear behaviour of the tangential force with applied load is observed. The change in slope of the curve indicates the detachment of the coating from the substrate. However, it is difficult to determine transition points in the above curve. The coefficient of friction  $\mu_{\text{eff}} = F_{\text{H}}/F_{\text{V}}$ , plotted against vertical load,  $F_{\text{V}}$ , yields a useful plot as shown in Fig. 6 (b). The plot clearly demonstrates a transition in the linear frictional behaviour of the  $\text{Al}_2\text{O}_3/\text{SiO}_2/\text{AISI 316L}$  system. The critical load determined on four samples was  $24 \pm 2$  N. Similar results for adhesion strength failure of  $\text{Al}_2\text{O}_3$  films have also been reported in literature [31,32]. Phani et al. [31] have

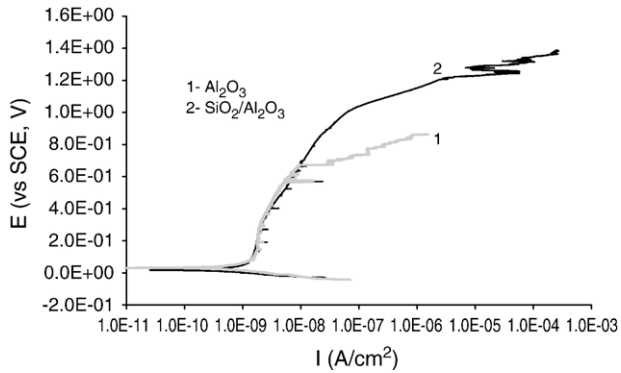


Fig. 7. Potentiodynamic polarization curves for coated AISI 316L in Ringer's solution at 25 °C.

deposited thin films of  $\text{Al}_2\text{O}_3$  on polished silica glass substrates by sol–gel dip-coating technique followed by annealing at 200–800 °C or exposure to microwave radiation at different powers. The critical load up to 25 N for adhesion strength failure has been reported for both annealed and microwave irradiated films.

### 3.2. Electrochemical characterization

Fig. 7 shows the potentiodynamic polarization behaviour of  $\text{Al}_2\text{O}_3$  coated AISI 316L at 25 °C with and without an intermediate layer of  $\text{SiO}_2$ . The presence of silica intermediate layer has shifted the breakdown potential of  $\text{Al}_2\text{O}_3$  coating from 670 mV to 1030 mV. The higher breakdown potential of silica alumina coating may be explained on the basis of much lower free energy values of alumina silica mixed compounds (such as  $-6901$  and  $-2616$   $\text{kJ mol}^{-1}$  for Mullite and Sillimanite, respectively) than boehmite ( $-985$   $\text{kJ mol}^{-1}$ ) alone [33]. The presence of  $\text{SiO}_2$  film between substrate and  $\text{Al}_2\text{O}_3$  coating would have produced a thermodynamically stabilized silica alumina interface that showed better stability against corrosion as compared to alumina alone [33]. Therefore, in all further studies, silica was coated on AISI 316L prior to alumina deposition.

The influence of final heat treatment of the coating on the polarization behaviour in Ringer's solution at 37 °C is shown in Fig. 8. The coating heated at 300 °C for 2 h showed a brief

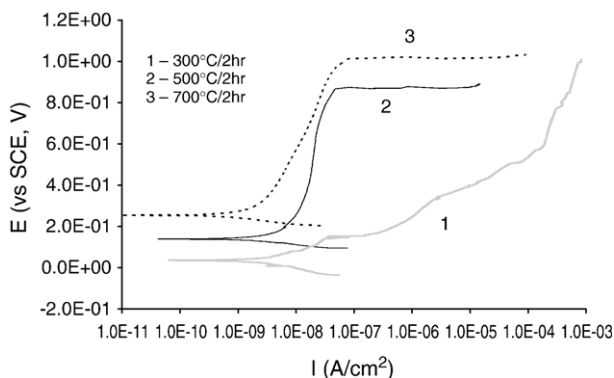


Fig. 8. Potentiodynamic polarization curves for  $\text{SiO}_2/\text{Al}_2\text{O}_3$  films on AISI 316L in Ringer's solution at 37 °C.

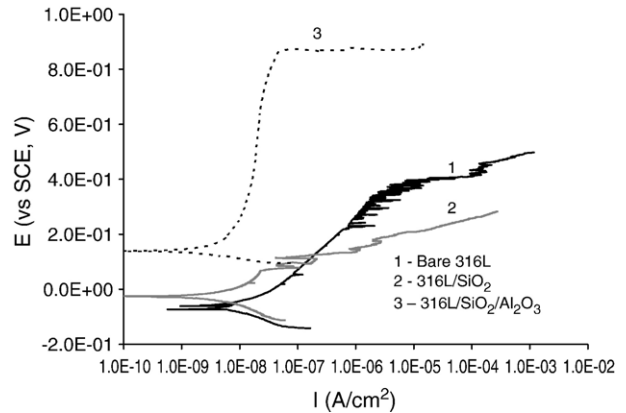
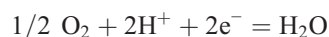


Fig. 9. Potentiodynamic polarization curves for coated and bare AISI 316L in Ringer's solution at 37 °C.

passivation (up to 153 mV) followed by gradual increase in current. Slow increase in current even up to 1.0 V, unlike faster increase above break down potential showed by uncoated substrate, indicates slow absorption of electrolyte through the pores in the oxide coating. The coatings heated at 500 °C and 700 °C for 2 h displayed barrier type of behaviour. Latter showed lower passivation current and breakdown potential higher by about 155 mV than that treated at 500 °C. The change in polarization behaviour with increase in final heat treatment temperature from 300 to 700 °C may be attributed to densification of the coating at higher temperatures. The reproducibility of the coating heated at 700 °C, however, was only 33%, unlike at 500 °C where coating was 100% reproducible. This probably would have been due to the formation of defects at higher temperature. The optimum temperature, therefore, was concluded to be 500 °C and was considered as a final heat treatment step for other studies.

The comparison of corrosion protection ability of the present coating with uncoated and only silica coated SS-316L is presented in Fig. 9. It appears that the silica coating alone was not dense enough to protect the substrate from corrosion. With the increase in anodic potential, the defects were created in the coating and caused breakdown potential to lower by about 310 mV, as compared to uncoated AISI 316L. Depositing  $\text{Al}_2\text{O}_3$  film on silica-coated steel and subsequent heating at 500 °C shifted the pitting potential of AISI 316L by 480 mV in noble direction.

The coating performance was also investigated in the Ringer's physiological solution at different pH — 4.0, 7.4, and 9.0. This was done as pH in the body has been reported to vary during surgery and also widely differs among various parts of the body [34]. The anodic polarization behaviour of coating was almost identical at three different pH values except that the shift of corrosion potential (155 mV) in positive side with decrease in pH to 4.0. More noble  $E_{\text{corr}}$  with decrease in pH from 7.4 to 4.0 may be explained by considering the pH dependent Nernst equation,  $E(V) = 1.23 - 0.059 \text{ pH}$ , of the following reaction:



It is clear from above equation that the decrease in pH will result in nobler redox potential of oxygen reduction which governs the corrosion kinetics in such solutions. Noble redox potential of  $O_2$  reduction will shift the corrosion potential of  $Al_2O_3$  coated AISI 316L in more positive direction.

The stability of the coating was checked by immersing the coated AISI 316L in solution for about an hour, so as to attain the stable OCP ( $\sim +260$  mV), followed by polarizing it anodically to  $+800$  mV (close to but below break down potential) and back to OCP. The polarization curve is shown in Fig. 10 (a). The same specimen, after polarization, was left in the solution for about 100 h to record any unusual fluctuations in the potential (OCP) due to peeling/dissolving of the coating. It was assumed that polarizing the coated AISI 316L to high anodic potential (such as close to the pitting potential) may destabilize the coating or metal/coating interface according to known film breakdown mechanism [35]. The OCP measurement for such a long time (100 h), however, did not show significant variation in OCP (Fig. 10b), indicating the coating yet intact. When the same specimen, was subjected again to polarization high in the anodic regions, the nature of the curve appeared to remain unchanged as shown in Fig. 10a. This observation, thus, confirms the stability or resistance of coating against any degradation in the aqueous medium.

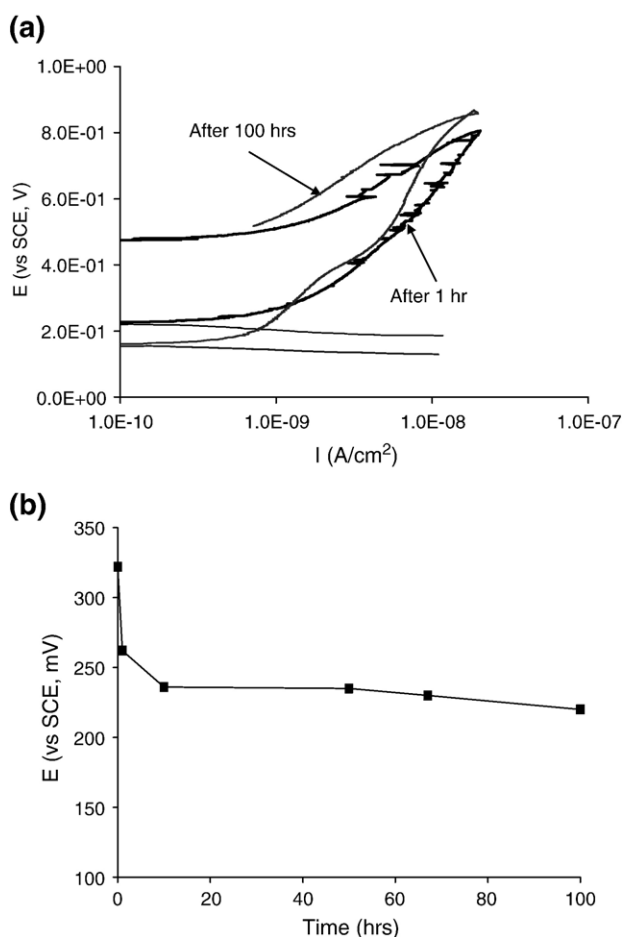


Fig. 10. Performance of  $SiO_2/Al_2O_3$  on AISI 316L as a function of immersion period in Ringer's solution at  $25^\circ C$ . (a) Polarization curves; (b) OCP variation.

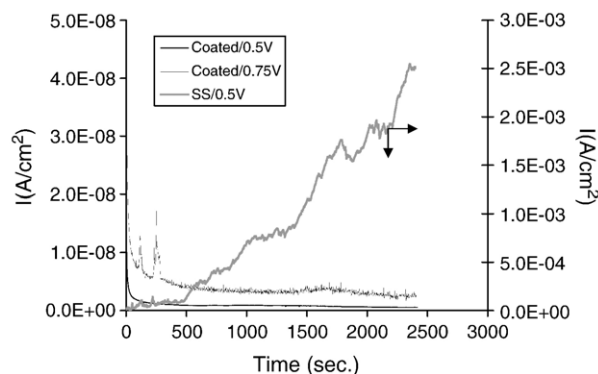


Fig. 11. Chronoamperometric evaluations of coated and bare SS316L in Ringer's solution at  $37^\circ C$ .

The release of deleterious metal ions was studied by allowing both bare and alumina coated AISI 316L to corrode at  $+500$  mV (above the pitting potential of bare AISI 316L) for 40 min. The potential was decided so as to produce significant amount of metal ions to compare the two specimens (coated and uncoated) in terms of their emitted ionic concentration. It is an important aspect of bio-implants that influences their performance and biocompatibility in the body. While corroding at  $+500$  mV, the resultant current was recorded till 40 min and shown in Fig. 11. The current was lower for coated electrode by six orders of magnitude than for uncoated one. The solutions in which samples were corroded were submitted for analyses (using ICP) to detect and measure the various metal ions (such as Fe, Cr, Ni and Mo). The quantities of metal ions leached out from uncoated electrode were: Fe  $\sim 0.073$  mg, Cr  $\sim 0.016$  mg, Ni  $\sim 0.008$  mg and Mo  $\sim 0.005$  mg, whereas no such metal ions were found from the solution from corrosion of coated AISI 316L. These results were compared with the blank solution (fresh Ringer's solution without exposing the coated or uncoated AISI 316L) where no such ions were noticed. Metal ions were absent in the solution after coated SS was forced to corrode at even higher anodic potential ( $+750$  mV) for 40 min. These results, however, support the application of  $SiO_2/Al_2O_3$  coating in preventing the unwanted metal ions from going into the body and hence suitable for bio-implants.

#### 4. Conclusion

A systematic study was made to develop corrosion resistant silica/alumina coating on AISI 316L for implant applications. The coating was homogeneous with thickness  $\sim 0.35 \pm 0.03$   $\mu m$  and showed significant scratch resistance. The pitting potential of AISI 316L after coating was shifted by about 470 mV towards positive side in physiological Ringer's solution. The change in pH did not influence the performance of the coating. The coated AISI 316L electrodes was stable and did not degrade after long time of exposure in the Ringer's solution. Coating was able to prevent the leaching of undesired metal ions from the substrate at even high anodic potential (up to  $+750$  mV), where bare AISI 316L released significant metal contents.

## Acknowledgement

The authors are grateful to the Director, National Metallurgical Laboratory, Jamshedpur for his encouragement and permission to publish this work.

## References

- [1] M. Sumita, T. Hanawa, S.H. Teoh, *Mater. Sci. Eng., C, Biomim. Mater., Sens. Syst.* 24 (2004) 753.
- [2] J. Brunski, in: B. Ratner, A. Hoffman, F. Schoen, J. Lemons (Eds.), *Biomaterial Science: An Introduction to Material in Medicine*, Academic Press, San Diego, 1996, p. 37.
- [3] M. Sumita, *Orthop. Surg.* 48 (1997) 927.
- [4] H. Placko, S. Brown, J. Payer, *J. Biomed. Mater. Res.* 17 (1983) 655.
- [5] M.A. Costa, M.H. Fernandes, *J. Mater. Sci., Mater. Med.* 11 (2000) 141.
- [6] P.K. Chu, J.Y. Chen, L.P. Wang, N. Huang, *Mater. Sci. Eng., R Rep.* 36 (2002) 143.
- [7] S. Mandl, B. Rauschenbach, *Surf. Coat. Technol.* 156 (2002) 276.
- [8] H. Schmidt, C. Konetschny, U. Fink, *Mater. Sci. Technol.* 14 (1998) 592.
- [9] H. Badekas, C. Panagopoulos, S. Ecomnomou, *J. Mater. Process. Technol.* 44 (1994) 54.
- [10] T.M. Yue, J.K. Yu, Z. Mei, H.C. Man, *Mater. Lett.* 52 (2002) 206.
- [11] R. Singh, N.B. Dahotre, *Surf. Eng.* 21 (2005) 297.
- [12] E. Gyorgy, A. Perez Del Pino, P. Sera, J.L. Merenza, *Surf. Coat. Technol.* 173 (2003) 265.
- [13] H.C. Man, N.Q. Zhao, Z.D. Cui, *Surf. Coat. Technol.* 192 (2005) 341.
- [14] A. Matthews, *Advances in surface processing technology*, in: K.M. Strafford, P.K. Data, J.S. Gray (Eds.), *Surface Engineering Practice*, Ellis Horwood Ltd, New York, 1990, p. 33.
- [15] C.E. Morosanu, *Thin Films by Chemical Vapour Deposition*, Elsevier, Amsterdam, 1990, p. 31.
- [16] M.C. Garcia-Alonso, L. Saldana, G. Valles, J.L. Gonzalez-Carrasco, J. Gonzalez-Cabrero, M.E. Martinez, E. Gil-Garay, L. Munuera, *Biomaterials* 24 (2003) 19.
- [17] B. Yang, M. Uchida, Hyun-Min Kim, X. Zhang, T. Kokubo, *Biomaterials* 25 (2004) 1003.
- [18] M. Guglielmi, *J. Sol-Gel Sci. Technol.* 8 (1997) 443.
- [19] K. Izumi, M. Murakami, T. Deguchi, A. Morita, *J. Am. Ceram. Soc.* 72 (1989) 1465.
- [20] W. Liu, Y. Chen, C. Ye, P. Zhang, *Ceram. Int.* 28 (2002) 349.
- [21] A. Balamurugan, S. Kannan, S. Rajeswari, *Mater. Lett.* 57 (2003) 4202.
- [22] P. Galliano, J.J. de Damborenea, M.J. Pascual, A. Duran, *J. Sol-Gel Sci. Technol.* 13 (1998) 723.
- [23] D.C.L. Vasconcelos, J.A.N. Carvalho, M. Mantel, W.L. Vasconcelos, *J. Non-Cryst. Solids* 273 (2000) 135.
- [24] J. Gallardo, A. Durán, J.J. de Damborenea, *Corros. Sci.* 46 (2004) 795.
- [25] M. Atik, P. de Lima Neto, L.A. Avaca, M.A. Aegerter, *Ceram. Int.* 21 (1995) 403.
- [26] J. Masalski, J. Gluszek, J. Zabrzski, K. Nitsch, P. Gluszek, *Thin Solid Films* 349 (1999) 186.
- [27] H.M. Hawthorne, A. Neville, T. Troczynski, X. Hu, M. Thammachart, Y. Xie, J. Fu, Q. Yang, *Surf. Coat. Technol.* 176 (2004) 243.
- [28] M. Natali, G. Carta, V. Rigato, G. Rossello, G. Salmaso, P. Zanella, *Electrochim. Acta* 50 (2005) 4615.
- [29] G. Urretavizcaya, A.L. Cavalieri, J.M. Porto López, I. Sobrados, J. Sanz, *J. Mater. Synth. Process.* 6 (1998) 1.
- [30] Chih-Peng Lin, Shaw-Bing Wen, *J. Am. Ceram. Soc.* 85 (2002) 1467.
- [31] A.R. Phani, S. Santucci, *J. Non-Cryst. Solids* 352 (2006) 4093.
- [32] T. Hübert, S. Svoboda, B. Oertel, *Surf. Coat. Technol.* 201 (2006) 487.
- [33] H. Schmidt, S. Langenfeld, R. Naß, *Mater. Des.* 18 (1997) 309.
- [34] K.J. Bundy, *Crit. Rev. Biomed. Eng.* 22 (1994) 139.
- [35] J.R. Galvele, in: R.P. Frankenthal, J. Kruger (Eds.), *Passivity of Metals*, The Electrochemical Society, Pennington, NJ, 1978, p. 285.